

Vacuum Decay in Time-Dependent Backgrounds

Patrick Draper¹, Manthos Karydas², and Hao Zhang³

Illinois Center for Advanced Studies of the Universe & Department of Physics,
University of Illinois, 1110 West Green St., Urbana IL 61801, U.S.A.

Abstract

We develop semiclassical methods for studying bubble nucleation in models with parameters that vary slowly in time. Introducing a more general rotation of the time contour allows access to a larger set of final states, and typically a non-Euclidean rotation is necessary in order to find the most relevant tunneling solution. We work primarily with effective quantum mechanical models parametrizing tunneling along restricted trajectories in field theories, which are sufficient, for example, to study thin wall bubble nucleation. We also give one example of an exact instanton solution in a particular Kaluza-Klein cosmology where the circumference of the internal circle is changing in time.

arXiv:2306.01609v1 [hep-th] 2 Jun 2023

¹pdraper@illinois.edu

²karydas2@illinois.edu

³haoz17@illinois.edu

1 Introduction

Almost fifty years ago, Coleman and collaborators developed powerful Euclidean path integral methods to compute vacuum decay rates in a semiclassical expansion [1–3]. The phenomenon is of clear cosmological and existential relevance, and continues to drive interesting theoretical work, most importantly the development of new calculational tools [4–14].

Euclidean path integral techniques are most straightforwardly applied to systems with time-independent couplings. However, if the tunneling field is coupled to other dynamically evolving fields, the tunneling potential may become effectively time dependent. In this paper we discuss generalizations of the semiclassical approach that can be used to compute tunneling probabilities in systems with time dependent parameters.

In Sec. 2 we describe a formulation of the semiclassical tunneling problem convenient for analyzing scenarios with explicit time dependence. The time dependence must be adiabatic, so that it makes sense to focus on the instantaneous semiclassical false and true vacua. The main differences with the usual Euclidean approach are (a) the introduction of a generalized time contour, and (b) a reformulation of the variational problem, from fixed initial position and fixed energy, to fixed wavepacket-like initial and final states at fixed times. Actually, the wavepacket formulation is mainly useful for interpreting the results of computations where the initial energy is still provided: it maps the real and imaginary parts of the initial and final momenta in the semiclassical solution to simple features of the initial and final packet wavefunctions.

In Sec. 3 we examine the role of the rotation angle of the time contour in time-independent systems. We find that adjusting this contour allows us to identify different final states outside the potential barrier, all related to each other by classical time evolution. Another way to view this is that the time contour controls the time at which barrier penetration begins. In Sec. 4 we turn to time-dependent systems, beginning with a toy model that can be solved analytically. In this case the generalized time contour turns out to be essential: controlled solutions are only obtained if the time contour is not too close to the Euclidean axis. Next we study thin-wall bubble nucleation in 3+1 dimensions with time dependent parameters. The leading correction to the semiclassical action can be obtained analytically, and solutions for the tunneling trajectories are easily obtained numerically. We describe how to make an optimal choice of continuation parameter depending on the path integral of interest.

In Sec. 5 we discuss gravitational effects. We outline a general treatment, then consider some particular cases where approximations can make the problem more tractable. We find, for example, that the leading $\mathcal{O}(H)$ contribution to the real part of the action vanishes for thin-wall nucleation on a fixed FRW background. We also describe, in Sec. 6, an example of a Kaluza-Klein cosmology where a full bubble solution for the fields can be obtained. In this case the Lorentzian bubble metric is real, but the instanton is quasi-Euclidean, corresponding to a complex metric.

Sec. 7 contains some comments on directions for further development.

2 Semiclassical Formulation

In the usual semiclassical treatment of vacuum decay, one searches for saddle points of the Euclidean path integral that interpolate between the false vacuum and a bubble of true vacuum, or in quantum mechanics, between the false vacuum and a point outside the well.

To get a different perspective on the problem, let us consider real-time quantum mechanical transition amplitudes of the form

$$\langle \psi_f(R, T_f) | \psi_i(R, T_i) \rangle = N \int dR_i dR_f \int_{R(T_i)=R_i}^{R(T_f)=R_f} DR e^{iS/\hbar},$$

$$S = S_i(R_i) - S_f(R_f) + \int_{T_i}^{T_f} dt L(\partial_t R, R, t). \quad (1)$$

The initial and final states are given by wavefunctions parametrized as $\psi(R) = e^{iS_{i,f}(R)/\hbar}$, where $S_{i,f}$ are complex functions. In tunneling problems these wavefunctions should be localized inside and outside of a false vacuum well. We have written explicit factors of \hbar to indicate that we are interested in states where both the real and imaginary parts of $S_{i,f}$ contain contributions of order one in the \hbar expansion, like coherent states, but subsequently we will drop the \hbar s. A similar starting point was used to study complexified path integral trajectories in [15].

Next, we perform a general rotation of the time contour, $t \rightarrow e^{i\gamma}\tau$. The Euclidean continuation corresponds to $\gamma = -\pi/2$, but it turns out to be useful to keep γ arbitrary. This technique was applied to the symmetric double well tunneling problem in [16].¹

After rotation of the time contour, the path integral appearing in the amplitude is

$$\int dR_i dR_f \int_{R(T_i)=R_i}^{R(T_f)=R_f} DR e^{-S_c},$$

$$S_c = -iS_i(R_i) + iS_f(R_f) - i \int_{T_i}^{T_f} d\tau L_c(\partial_\tau R, R, \tau)$$

$$L_c(\partial_\tau R, R, \tau) = e^{i\gamma} L(e^{-i\gamma} \partial_\tau R, R, e^{i\gamma} \tau). \quad (2)$$

In the leading semiclassical approximation we are interested in solutions to the the bulk Euler-Lagrange equation, $\delta L_c / \delta R - \partial_\tau (\delta L_c / \delta \partial_\tau R) = 0$. The equation of motion can be replaced by the conservation of energy condition if L does not depend explicitly on t .

Finally, since we have introduced general initial and final states, the variational problem

¹Among the interesting phenomena observed in [16] is that the ordinary Euclidean instanton, with a hyperbolic tangent profile, becomes a complex space-filling curve in the real-time limit $\gamma \rightarrow 0$. γ will play a somewhat different role in the decay problems considered here.

gives rise to boundary conditions:

$$\begin{aligned} p_i &\equiv \left. \frac{\delta L_c}{\delta \partial_\tau R} \right|_{\tau=T_i} = S'_i(R_i) \\ p_f &\equiv \left. \frac{\delta L_c}{\delta \partial_\tau R} \right|_{\tau=T_f} = S'_f(R_f). \end{aligned} \quad (3)$$

Eq. (3) will be important for understanding the various semiclassical tunneling solutions we obtain below. These conditions relate the initial and final momenta of the semiclassical trajectories to the gradient of the wavefunction at the initial and final positions.

At leading order in the semiclassical expansion, the task is to solve the equations of motion subject to the boundary conditions (3). The canonical variables in the solution are generally complex-valued. In addition to the $e^{i\gamma}$, $S_{i,f}$ are complex if, say, the states defined on real $R_{i,f}$ are modeled as Gaussian wavepackets or some similar perturbative ground state. To estimate a total decay probability, one must also extremize over semiclassically inequivalent final states, and integrate over any zero modes.

Although this is an acceptable formulation of a tunneling problem, generally it is not what is done in standard, time-independent tunneling problems. One instead solves a variational problem with fixed energy:

$$E_E = E_{FV} \quad (4)$$

where E_E is the Euclidean energy and $E_{FV} = V(R_{FV})$ is the value of the potential in the classical false vacuum R_{FV} . Typically there is a solution to Eq. (4) that starts at R_{FV} and reaches the classical turning point $R = R_{TP}$ with zero momentum at some later time, which is determined by the solution. For example, in an inverted quartic double well model,

$$L = \frac{1}{2}\dot{R}^2 - R^2 + \lambda R^4, \quad (5)$$

the relevant zero-energy Euclidean solution is

$$R = \frac{1}{\sqrt{\lambda}} \operatorname{sech}(\sqrt{2}\tau). \quad (6)$$

(In this case R_{FV} and R_{TP} are only reached asymptotically, but this is not important.)

From such a solution, we may work backward and identify problems of the type (1)-(3) to which it is also a solution. In a corresponding problem of the type (1)-(3), one needs a low-energy initial state, like the perturbative ground state wavefunction in the false vacuum, for which $S'_i(R_{FV}) = 0$, and similarly the final state can be some zero-momentum wavepacket peaked at R_{TP} . These requirements are typical of time-independent problems analytically continued to Euclidean time.

We will see that other final states arise naturally in two more general situations: first, we consider time-independent problems with arbitrary time continuation parameters γ , and second, cases with explicit time-dependence in the action. We solve the semiclassical equa-

tions of motion with initial energy as input, finding trajectories that end, typically, at some $R_f \neq R_{TP}$ with $p_f \neq 0$. From these solutions we may read off amplitudes of the form (1) for which they also provide saddle point trajectories. In particular Eq. (3) provides relations between the complex semiclassical momenta and features of suitable wavepackets.

Let us pause and make a couple of tangential comments. First, in relating a complex-time solution to the original real-time amplitude (1), there is a little more that needs to be said about the continuation of the parameters $T_{i,f}$ back to real time. We will discuss this issue below. Second, we note that it is important *not* to consider a path integral with fixed initial and final times and fixed initial and final values of R . Position eigenstates have completely uncertain momentum, and there will always be solutions, unrelated to tunneling, that have enough energy to summit the barrier classically. The fixed-energy formulation avoids these complications, as does the wavepacket formulation, as long as the gradients in the wavepacket are not too large.

3 Time-Independent Tunneling with $t \rightarrow e^{i\gamma}\tau$

In this section we consider the general Wick rotation with parameter γ . For illustration, we work with examples of the form

$$L = -R_0 R^{p-1} \sqrt{1 - (\partial_t R)^2} + R^p. \quad (7)$$

A large class of field theoretic vacuum decay processes are described by this effective Lagrangian at the leading semiclassical order, including thin-wall bubble nucleation in $d = p$ spatial dimensions, Schwinger pair production in a constant background electric field for $p = 1$, and bubble of nothing decays for $p = d - 1$. (Therefore R is assumed to be ≥ 0 , since it plays the role of a radial collective coordinate.) For example, consider a real scalar field in 3+1 dimensions with a double-well potential and a small symmetry breaking parameter ϵ ,

$$V(\phi) = \frac{1}{2}\lambda(\phi^2 - a^2)^2 - (\epsilon/2a)\phi. \quad (8)$$

It is well-known that the effective theory (7) with $p = 3$ is obtained from a Born-Oppenheimer approximation to the Klein-Gordon field theory with potential (8). Let us briefly review the construction which will be useful to have in mind when we include slow time dependence.

For small ϵ the semiclassical states relevant for tunneling in the theory (8) are large spherical domain walls. Neglecting the slow accelerations driven by curvature and the energy gap ϵ , the equation of motion for the “heavy” degrees of freedom is $\partial_t^2 \phi - \partial_r^2 \phi + 2\lambda(\phi^2 - a^2)\phi = 0$, for which the relevant solutions are

$$\phi \approx a \tanh \left[\frac{\sqrt{\lambda}a(R + vt - r)}{\sqrt{1 - v^2}} \right]. \quad (9)$$

Here R is a large radius, v is the wall velocity, the wall tension is given by $\sigma \propto \sqrt{\lambda}a^3$, and the

factor of $\frac{1}{\sqrt{1-v^2}}$ accounts for length contraction of the wall thickness. To obtain an effective action for slow variations of v driven by curvature and pressure, we replace $R + vt \rightarrow R(t)$, $v \rightarrow \dot{R}(t)$, and plug these field configurations into the Klein-Gordon action. Upon so doing each term in the Lagrangian is found to be proportional to $f(r) \operatorname{sech}^4 \left[\frac{\sqrt{\lambda} a (R-r)}{\sqrt{1-\dot{R}^2}} \right]$. In the thin-wall limit $\frac{\sqrt{\lambda} a}{\sqrt{1-\dot{R}^2}} R \gg 1$ the sech^4 is sharply peaked around $r = R$, so we may replace $f(r) \rightarrow f(R)$ and do the integral over space. One obtains an effective Lagrangian for the collective coordinate $R(t)$ which is, apart from an overall multiplicative constant, given by Eq. (7) with $p = 3$ and $R_0 = 3\sigma/\epsilon$. (We will be lax about such multiplicative constants, which do not affect the equations of motion and can be restored easily in the on-shell action.)

Since (7) does not depend explicitly on time, there is a conserved energy. After continuation $t \rightarrow e^{i\gamma}\tau$, the conserved energy is

$$E = e^{i\gamma} \left(\frac{R_0 R^{p-1}}{\sqrt{1 - e^{-2i\gamma} (\partial_\tau R)^2}} - R^p \right). \quad (10)$$

There is a false vacuum at $R_{FV} = 0$ with $E_{FV} = 0$, and the classical turning point is $R_{TP} = R_0$. It is also informative to write the energy in terms of the momentum $P = e^{-i\gamma} R_0 R^{p-1} (\partial_\tau R / \sqrt{1 - e^{-2i\gamma} (\partial_\tau R)^2})$,

$$E = e^{i\gamma} \left(\sqrt{P^2 + R_0^2 R^{2(p-1)}} - R^p \right). \quad (11)$$

For $p > 1$, $T_f = 0$, and sufficiently early T_i , the solutions to Eq. (4) relevant for tunneling are quite simple. In the Euclidean case $\gamma = -\pi/2$, they are

$$R = \Theta(\tau + R_0) \sqrt{R_0^2 - \tau^2}. \quad (12)$$

The solution is real in the relevant range of τ , and the nucleation point is $R(0) = R_0$, where the momentum vanishes. For other γ , R is generally not real, so we seek a zero energy solution for which R is real at $\tau = 0$. Eq. (12) generalizes to

$$R = \Theta(\tau - R_0 \csc \gamma) \sqrt{R_0^2 + (e^{i\gamma} \tau - R_0 \cot \gamma)^2}. \quad (13)$$

The particle sits at the $R = 0$ false vacuum until $\tau = \tau_0 \equiv R_0 \csc \gamma$, then moves in the complex R plane to the nucleation point at $\tau = 0$,

$$R(0) = R_0 |\csc \gamma|. \quad (14)$$

Curiously, the nucleation point only coincides with the classical turning point in the Euclidean case. Examples are shown in Fig. 1.

We should say a word about the sense in which Eqs. (12), (13) are saddle points of the action. Since \dot{R} is not defined at $\tau = \tau_0 = R_0 \csc \gamma$, we must give it a definition so that the

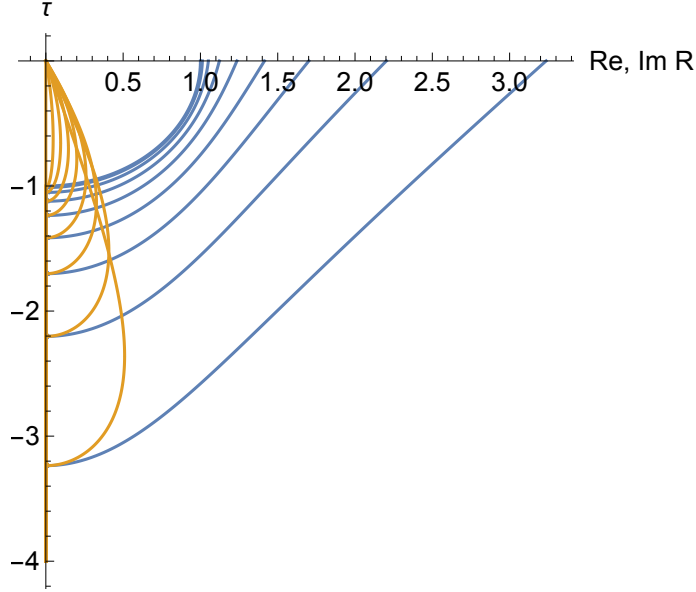


Figure 1: Tunneling trajectories (13) with $R_0 = 1$ and a range of γ between $-\frac{\pi}{2}$ (Euclidean) and $-\frac{\pi}{10}$. As $\gamma \rightarrow 0^-$ the tunneling starts earlier and ends further outside the well, with finite classical momentum such that the total energy is conserved.

trajectories are in the domain of the action functional. Any definition of \dot{R} as a discontinuous function is sufficient and results in the same value of the action. The discontinuity in \dot{R} gives rise to a delta distribution in \ddot{R} , which could spoil the stationarity of the action under variations. However, for $p > 1$ the delta function is multiplied by a positive power of R in the action density, which vanishes at $\tau = R_0 \csc \gamma$.

We have assumed that the initial time is early enough, $T_i < R_0 \csc \gamma$, so that the instanton can “fit.” Apart from this constraint, the action of the semiclassical solution is independent of T_i . The particle sits as long as it needs to in the false vacuum, and then at $\tau = R_0 \csc \gamma$ it starts the jump to the nucleation point.

To better understand the solutions for $\gamma \neq -\pi/2$, we can ask what wavepacket problems of the form (1)-(3) they also solve. Let us examine the boundary conditions (3). The final momentum of the solutions (13) is

$$p_f = -R_0^p |\csc \gamma|^{p-1} \cot \gamma. \quad (15)$$

In particular, it is real, and so is related to the gradient of the phase of the final wavefunction by Eq. (3). For wavepackets the gradient of the phase is just the classical momentum P .

Furthermore it is easily seen that the *real-time* energy, Eq. (11) with $\gamma = 0$, vanishes for all final states labeled by the real positions $R \rightarrow R(0)$ given in Eq. (14) and real momenta $P = p_f$ given in Eq. (15). This is because Eq. (11) only depends explicitly on γ in an overall multiplicative factor, and Eq. (3) instructs us to map the semiclassical trajectory momentum p_f and the semiclassical final state momentum P to each other. The final states at $\tau = 0$ correspond to different points in phase space, related by real-time classical evolution.

We conclude that different values of γ correspond to equivalent tunneling processes in an interesting way. For $-\pi < \gamma < -\pi/2$, the classical state is a particle somewhere to the right of the potential barrier, moving up the hill toward the classical turning point. For $-\pi/2 < \gamma < 0$, the particle is moving away from the turning point. Classical evolution, either forward or backward in time, takes the particle to the state at rest at the turning point, which is the nucleation point for $\gamma = -\pi/2$. We may interpret this as meaning that different γ (in the range $-\pi/2 < \gamma < 0$) correspond to different times at which a bubble nucleates at rest. The semiclassical path integral computes the amplitude to evolve from “no bubble” at T_i to “some bubble” at T_f , and different γ appear to naturally account for the fact that we would also find a nonzero semiclassical amplitude, to nucleate a bubble with a smaller p_f , if we chose earlier T_i .

Consistent with this interpretation, all of the trajectories have the same on-shell value of the real part of the action. For example, for $p = 3$, one finds

$$\text{Re} \left[-i \int_{T_i}^{T_f} d\tau L_c(\partial_\tau R, R, \tau) \right] = \frac{\pi R_0^4}{16} \quad (16)$$

independent of γ .

According to Eq. (2), the tunneling exponent $\text{Re}(S_c)$ also receives contributions from the initial and final state via $\text{Im}(S_{i,f}(R_{i,f}))$. These factors can also be taken to be independent of γ . For example, the final states can be chosen as wavepackets related by translation in R . (As long as the packets are localized away from the origin, the fact that R is bounded from below is of no practical consequence.)

Finally, we must consider the analytic continuation of the amplitude back to real time. This is different from taking the limit $\gamma \rightarrow 0$ in the semiclassical solutions, because we have identified solutions with different values of γ as saddle points describing tunneling between different final states. Instead we want to continue the amplitude in the complex T_i -plane back to the real time axis, for *fixed* final states. Here we will be content with a plausibility argument. We have already seen that for fixed γ the tunneling exponent is independent of T_i (if $|T_i| > R_0 |\csc \gamma|$, so that the trajectory described by the instanton has enough time to complete.) Furthermore on physical grounds the real time decay rate is expected to be constant over timescales long compared to the perturbative timescales in the false vacuum and short compared to the lifetime. Therefore we make the plausible assumption that T_i can be continued back to the real axis, trivially, for any final state corresponding to some γ . Furthermore we have seen that we obtain the same real part of the exponent, which controls the lifetime, for any γ .

4 Time-Dependent Tunneling

The formulations of the tunneling problem described above admit a straightforward generalization to time-dependent systems. We consider two explicit examples, a toy model and thin-wall bubble nucleation in 3+1 dimensions.

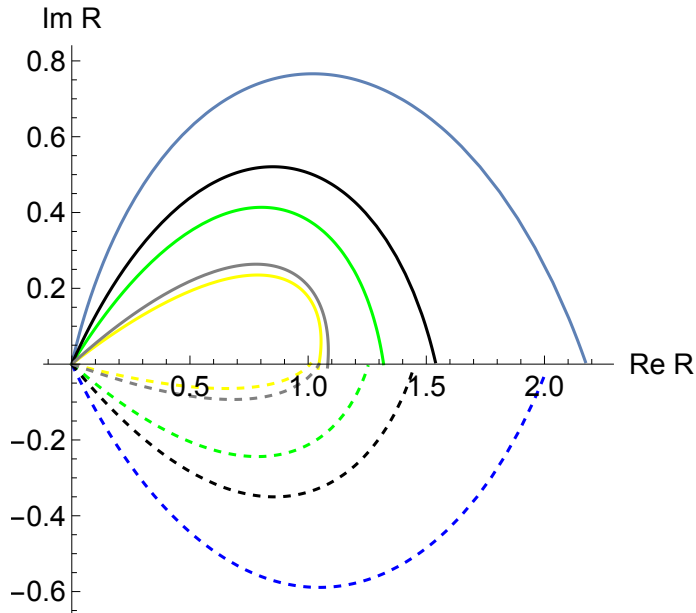


Figure 2: Tunneling trajectories (18) with $R_0 = 1$, $v = 1/20$, and a range of γ between $-\frac{\pi}{6}$ and $-\frac{2\pi}{3}$.

4.1 Toy model

The first example is simple enough that we can solve it more or less analytically:

$$L = (\partial_t R)^2 - ((R_0 + vt)R - R^2). \quad (17)$$

As before the degree of freedom is constrained to $R \geq 0$, so that on the domain of R , the classical potential has a false vacuum at $R = 0$. We assume $v > 0$ so that the barrier is growing with time. We are free to choose the time parametrization so that the nucleation time is $T_f = 0$, and we assume that R_0 is large enough so that $R_0 + vT_i > 0$. The model (17) has been scaled so that time is dimensionless and v has the dimensions of R .

We perform the same general continuation as previously, $t \rightarrow e^{i\gamma}\tau$, and seek solutions to the equations of motion on which the classical Hamiltonian vanishes at some $\tau = \tau_0$. The tunneling solution is

$$R(\tau) = \frac{1}{2} (R_0 + e^{i\gamma}\tau v) - \frac{1}{2} (R_0 + e^{i\gamma}\tau_0 v) \cosh(e^{i\gamma}(\tau - \tau_0)) - \frac{1}{2} v \sinh(e^{i\gamma}(\tau - \tau_0)). \quad (18)$$

Some examples are shown in the complex- R plane in Fig. 2.

To understand the decay process described by the solutions (18), we must determine the tunneling time, the relevant initial and final states, and the real part of the on-shell action. We consider each in turn.

Demanding that R is real again at $\tau = T_f = 0$ determines the tunneling time τ_0 via the

somewhat messy relation

$$R_0 \sin(\tau_0 \sin \gamma) \sinh(\tau_0 \cos \gamma) = v \left(\sin(\tau_0 \sin \gamma) \cosh(\tau_0 \cos(\gamma)) - \tau_0 [\sin \gamma (\cos(\tau_0 \sin \gamma)) \cosh(\tau_0 \cos \gamma) + \cos \gamma \sin(\tau_0 \sin \gamma) \sinh(\tau_0 \cos \gamma)] \right) \quad (19)$$

For nonzero v and Euclidean time, $\gamma = -\pi/2$, (19) reduces to $\tan(\tau_0) = \tau_0$, which has no nontrivial solution. Conversely it is satisfied by any τ_0 if $v = 0$ and $\gamma = -\pi/2$. We solve it perturbatively in small v :

$$\tau_0 = \pi \csc \gamma \left(1 - \frac{v}{R_0} \coth(\pi \cot \gamma) + \mathcal{O}(v^2) \right) \quad (20)$$

where the higher order coefficients are lengthy but easily calculable. Near $\gamma = -\pi/2$, the solution (20) behaves as

$$\tau_0 \sim - \left(\pi + (1/6 + \pi^2) \frac{v^2}{\pi R_0^2} \right) - \frac{v}{R_0} \left(\gamma + \frac{\pi}{2} \right)^{-1} + \frac{v^2}{\pi R_0^2} \left(\gamma + \frac{\pi}{2} \right)^{-2} + \dots \quad (21)$$

so the small- v expansion is only controlled for

$$|\gamma + \pi/2| \gg \frac{v}{\pi R_0}. \quad (22)$$

It is also possible to obtain τ_0 as an expansion in $\gamma + \pi/2$ for fixed nonzero v , but one finds that R_f is small, of order $\gamma + \pi/2$, and the solutions typically do not describe tunneling out of the well. In other words, we find the surprising property that in this problem we must not work too close to the imaginary time axis in order to obtain classical solutions relevant for tunneling.

Now we examine the initial and final states. To describe tunneling between two fixed times, we set $R = 0$ for $T_i \leq \tau \leq \tau_0$, and R is given by Eq. (18) for $\tau > \tau_0$. Despite its piecewise nature, it is easy to check that this trajectory is still a genuine stationary point of the continued action.² As for the final state, we find an $\mathcal{O}(v)$ correction to the nucleation point,

$$R_f(0) = R_0 + \frac{1}{2} R_0 (\cosh(\pi \cot \gamma) - 1) - \frac{1}{2} v \sinh(\pi \cot \gamma) + \dots \quad (23)$$

The $v = 0$ contribution exhibits the same behavior as the time-independent model of the previous section: as $\gamma \rightarrow 0^-$ it diverges, indicating nucleation far outside the barrier. On

²Actually, by constructing a model simple enough to solve analytically, we have inadvertently complicated this step, because the potential is not differentiable at the origin. Its derivative must be defined to be discontinuous, set to zero for all t at $R = 0$, and $R_0 + vt - 2R$ for $R > 0$. This is necessary for the vacuum solution $R = 0$ to exist. This technical complication will not arise in the bubble nucleation problem considered in the next section.

the other hand, near the Euclidean time axis (keeping leading terms of order v^2),

$$R_f(0) = R_0 + \frac{(5\pi^2 - 2)v^2}{24R_0} + \frac{1}{2}v\pi(\gamma + \pi/2) - \frac{v^2}{4R_0}(\gamma + \pi/2)^{-2} + \dots \quad (24)$$

The third term is negative if $\gamma < -\pi/2$ and the fourth term is negative definite. The second term is positive but for $|\gamma + \pi/2| \gg v/(\pi R_0)$ the third term is larger in absolute value so the sum of two is also negative. Within the small- v approximation, all of these terms must be much smaller in magnitude than R_0 . So a novel feature of time dependent systems, which do not conserve energy, is that it is possible to obtain a nucleation point less than the classical turning point at the nucleation time. However, in the present model this effect is atypical and marginal in the small- v expansion.

The final momenta of the trajectories are

$$\begin{aligned} \text{Re}(p_f) &= -R_0 \sinh(\pi \cot \gamma) + \mathcal{O}(v) \\ \text{Im}(p_f) &= \pi v \text{csch}(\pi \cot \gamma) + \mathcal{O}(v^2). \end{aligned} \quad (25)$$

As before, the final state is characterized by a nonzero classical momentum $\text{Re}(p_f)$ for general γ . The new feature is a nonzero imaginary component of p_f for nonzero v . For typical γ not too close to the Euclidean limit, $\text{Im}(p_f)$ is exponentially small, of order $ve^{-\pi/\gamma}$. $\text{Im}(p_f)$ is related to the gradient of the final-state wavepacket at the nucleation point, in problems of the type (1), by Eq. (3). The imaginary part of S_f and its gradient, for a wavepacket peaked at some R_* , satisfy

$$\begin{aligned} \text{Im}(S_f) &= (R_f - R_*)^2/2\sigma^2, \\ \text{Im}(S'_f) &= (R_f - R_*)/\sigma^2. \end{aligned} \quad (26)$$

A typical size of σ is $\lesssim \text{Re}(p_f^{-1})$. Consequently the typical distance from R_f to the peak of the wavepacket, for $|\gamma| \lesssim \mathcal{O}(1)$, is also exponentially small in π/γ . So to a good approximation we can still think of the final state as being peaked at R_f , if γ is not too close to the Euclidean limit, and the state possesses finite classical momentum.

In the opposite limit, close to Euclidean time (while maintaining the bound (22)), the classical momentum of the final state $\text{Re}(p_f)$ goes to zero like $\gamma + \pi/2$: the particle nucleates approximately at rest. The gradient of the final state wavefunction at the nucleation point grows like $(\gamma + \pi/2)^{-1}$: the stationary point of the wavepacket problem balances a decrease in the tunneling distance against a decrease in the amplitude of the final state wavefunction.

The decay amplitude is governed by the real part of the on-shell action,

$$\text{Re } S_c = \text{Im } S_i(0) - \text{Im } S_f(R_f) + \frac{\pi R_0^2}{4} + \frac{1}{2}\pi^2 R_0 v \cot(\gamma) + \mathcal{O}(v^2). \quad (27)$$

The first two terms depend on the wavepackets at the starting and nucleation points. Since typical semiclassical solutions permit $R = 0$ and $R = R_f$ to lie close to the packet peaks, these terms may be neglected. (There is a contribution from the wavefunction normalizations, but it is of higher order in the \hbar expansion.) The rest of (27) corresponds to the real part of the

action $\text{Re}(-i \int L_c d\tau)$ evaluated on the semiclassical trajectory.

The leading term in the v expansion, $\pi R_0^2/4$, corresponds to the time-independent semiclassical action. The $\mathcal{O}(v)$ correction can actually be computed just from the $\mathcal{O}(v)$ term in the action, evaluated on the $v = 0$ solution. This is not completely obvious because the perturbation also changes the solution at the initial and final times, as well as the initial time. The full perturbation to the on-shell action at order v takes the form:

$$\Delta S_c = v \left[\left(i e^{2i\gamma} \int_{\tau_0}^0 d\tau \tau R \right) + (i L_c(R, \tau = \tau_0) \partial_v \tau_0) + (i p \partial_v R) \right]_{\tau=\tau_0}^{\tau=0} \Big|_{v=0} \quad (28)$$

The second term arises from the $\mathcal{O}(v)$ correction to the initial time τ_0 . It vanishes because $L_c = 0$ at the initial time for $v = 0$. The third term involves the momentum $p = 2e^{-i\gamma} \partial_\tau R$. It arises from the integration by parts in the kinetic term when the on-shell action is varied with respect to v . Physically, it translates the initial and final R by $\delta R = v \partial_v R$. The $\tau = \tau_0$ contribution from this term vanishes because $\partial_\tau R$ vanishes at the initial time. The contribution from $\tau = 0$ is nonzero, but purely imaginary because p_f is real for $v = 0$. (Of course, these boundary variations must also cancel if Eq. (3) is satisfied.) Thus the first, “bulk” term in (28) accounts for the full $\mathcal{O}(v)$ term in (27), as can be verified explicitly,

$$\Delta \text{Re} S_c|_{\mathcal{O}(v)} = \frac{1}{2} \pi^2 R_0 v \cot(\gamma). \quad (29)$$

Physically, the $\mathcal{O}(v)$ correction to the tunneling exponent is sourced by several effects. First, the tunneling takes place at earlier times, when the potential barrier was smaller by an amount of order $R_0 v \csc \gamma$. (Recall that we assume $v > 0$, so that the barrier is growing in time; it is straightforward to reinterpret for negative v .) This effect decreases the action. Second, the tunneling duration $|\tau_0|$ (cf. Eq. (20)) has a $\mathcal{O}(v)$ correction, which also affects the action at $\mathcal{O}(v)$. The duration is longer for $\gamma < -\pi/2$, increasing the action, and shorter for $\gamma > -\pi/2$, further decreasing it. The net $\mathcal{O}(v)$ shift in the action is positive for $\gamma < -\pi/2$ and negative for $\gamma > -\pi/2$.

The magnitude of the $\mathcal{O}(v)$ contribution appears to decrease (increase) without bound as $\gamma \rightarrow 0^-$ ($\gamma \rightarrow -\pi^+$), in both cases because τ_0 is diverging to $-\infty$. This reflects two related facts. First the v expansion of the action breaks down at large $\tau_0 \sim R_0/v$, and so (27) is not reliable unless $\gamma \ll -\pi v/R_0$ and $\gamma \gg \pi + \pi v/R_0$. Then the correction is under control and the real part of the action is positive definite. Second, we should incorporate the bounds $R_0/v > |T_i| > |\tau_0|$, so that the tunneling processes have time to complete, and the barrier is already present at the initial time T_i when the system was known to be in its vacuum state. This implies the constraint $\pi v |\csc \gamma| < R_0$ for small v , which limits γ in the same way.

Apart from these bounds, what γ should we pick? The smallest action arises when tunneling starts right away, so that $T_i = \tau_0$ and the barrier is minimized. For small v this means we have $\pi \csc \gamma \approx T_i$. Then we find

$$\Delta \text{Re} S_c|_{\mathcal{O}(v), \max} = -\frac{1}{2} \pi R_0 v \sqrt{T_i^2 - \pi^2} \quad (30)$$

for any $-\pi > T_i > -R_0/v$. The upper bound on T_i requires that at least one instanton “fits” before the nucleation time $T_f = 0$, and the lower bound on T_i corresponds to the time when the barrier vanishes; note that here the correction to the action is of the same order as the leading term and of opposite sign.

The correction (30) is straightforward to understand. Part of the effect is translating the coupling R_0 appearing in the leading time independent action, $\frac{\pi}{4}R_0^2$, back to the starting time, $R_0 \rightarrow R_0 - vT_i$, at first order in v . This effect is dominant if $T_i \gg \pi$. The rest of the correction is the leading effect of time dependence while the particle is moving under the barrier. It vanishes in the Euclidean case, $T_i = \pi$, because here there is an extra $-i\tau$ in the $\mathcal{O}(v)$ Lagrangian, which makes the contribution purely imaginary.

As we found in the time-independent case, generic values of γ correspond to bubbles in motion at $T_f = 0$. As in the time-independent case it is natural to conclude that the solution is telling us that nucleation has effectively already occurred at an early time: we can evolve the characteristic position and momentum of a suitable wavepacket backward in real time to a state of smaller momentum closer to the classical turning point at that time. Our path integral only “asks” about events at T_f , but it “knows” about decays that occurred earlier.

Holding γ fixed, the on-shell action Eq. (27) is independent of T_i as long as the instanton fits. Therefore we may trivially continue the semiclassical amplitude e^{-S_c} back to real time, $T_{i,f} \rightarrow e^{-i\gamma}T_{i,f}$. This continuation only acts nontrivially on T_i , since $T_f = 0$.

We conclude that the solutions (18) provide a semiclassical approximation to the probability amplitude (1), with some low-energy initial state peaked at $R = 0$ at a specified initial time, and a final wavepacket localized near R_f at $T_f = 0$, with properties related to the real and imaginary parts of the final momentum by Eq. (3). As before, we have avoided the more difficult problem of solving the boundary value problem (3) with specified $S_{i,f}$ directly, and instead solve the initial value problem with specified R and \dot{R} . The price is that we did not know exactly what family of wavepacket transition amplitudes we solved until we computed the total tunneling time, the nucleation point, and final momentum of the solution.

4.2 Thin-wall bubble nucleation

Our second example is the 3+1 dimensional thin-wall bubble nucleation model. We consider the case of a time-dependent domain wall tension proportional to $\sigma(t)$ and vacuum energy splitting $\epsilon(t)$ (as before, geometric factors have been absorbed to reduce clutter):

$$L = -\sigma(t)R^2\sqrt{1 - (\partial_t R)^2} + \epsilon(t)R^3. \quad (31)$$

We assume that $\sigma(t)$, $\epsilon(t)$ are positive for all relevant times.

Before analyzing the tunneling processes in this model, let us discuss how (31) might arise as an effective action in a field theory coupled to a dynamical sector. For example, we can weakly couple the model (8) to another scalar χ rolling in a shallow potential,

$$V(\phi, \xi) = \frac{1}{2}\lambda(\phi^2 - a^2)^2 - \frac{\epsilon_0}{2a}(1 + g\chi/a)\phi + V(\chi). \quad (32)$$

Suppose that on the timescales of interest we can linearize $V(\chi) \approx c/a\chi$. The specifications of “weak coupling” and “shallow potential” mean we take the hierarchy $\lambda a^4 \gg (c\chi/a, \epsilon_0) \gg g\epsilon_0\chi/a$ over all relevant χ . Then we can add the effects of χ to the Born-Oppenheimer treatment described in Sec. 3. In the first step, we solve the approximate “heavy” dynamics, obtaining the profile (9) at zeroth order in ϵ_0 , c , and $1/R^2$. Subsequently we take the thin-wall limit. Then we obtain the “light” dynamics, finding a homogeneous rolling solution for χ at leading order in the hierarchy $c \gg g\epsilon_0$,

$$\chi = \chi_0 + vt + \frac{1}{2}(c/a)t^2, \quad (33)$$

for some χ_0 and v . Evaluating the Lagrangian on the thin-wall profile and Eq. (33) and integrating over space, we obtain the quantum mechanical model (31) with constant $\sigma = 16\pi\sqrt{\lambda}a^3/3$ and $\epsilon(t) = 4\pi/3[\epsilon_0 + (g/a)(\chi_0 + vt + \frac{1}{2}ct^2)]$.

With other weak couplings and potentials we may obtain arbitrary functions $\sigma(t)$ and $\epsilon(t)$, and possibly more general couplings. It is also straightforward to include backreaction of the ϕ profile on χ in the matching of the effective parameters, although this is higher order in g and may be subleading to corrections to the thin-wall limit.

Now let us study the tunneling solutions of (31), along the same lines as our analysis of the toy model. Unfortunately, in the present model, typically an analytic solution is no longer available. However, it is straightforward to construct numerical solutions, and the correction to the tunneling exponent may be obtained analytically when the parameters vary slowly.

To construct numerical solutions we require initial conditions. At early times the relevant nontrivial solutions behave as

$$\begin{aligned} R &= c\sqrt{\tau - \tau_0} (1 + \mathcal{O}(\tau - \tau_0)) , \\ c &= ie^{i\gamma/2} \sqrt{\frac{6(\sigma_0 + e^{i\gamma}\tau_0 v_\sigma)}{3i(\epsilon_0 + e^{i\gamma}\tau_0 v_\epsilon) + v_\sigma}} \end{aligned} \quad (34)$$

where $v_{\sigma,\epsilon}$ are defined by the early time expansions

$$\begin{aligned} \sigma(e^{i\gamma}\tau) &= \sigma_0 + e^{i\gamma}v_\sigma(\tau - \tau_0) + \dots, \\ \epsilon(e^{i\gamma}\tau) &= \epsilon_0 + e^{i\gamma}v_\epsilon(\tau - \tau_0) + \dots \end{aligned} \quad (35)$$

Using (34) as initial data, we may integrate the equations of motion with specified $\sigma(t)$, $\epsilon(t)$ until R becomes real again, which defines a nucleation point R_f . We may adjust τ_0 so that the nucleation time is $T_f = 0$. Call such a solution $\hat{R}(\tau)$. As before, we can also attach an arbitrary period of the solution $R = 0$ to the beginning of the solution $\hat{R}(\tau)$ to obtain a tunneling solution of longer total duration,

$$R(\tau) = \theta(\tau)\hat{R}(\tau); \quad T_i < \tau < 0. \quad (36)$$

In Fig. 3 we show example trajectories in a model with linear time dependence in σ and ϵ , such that the barrier height grows linearly in time.

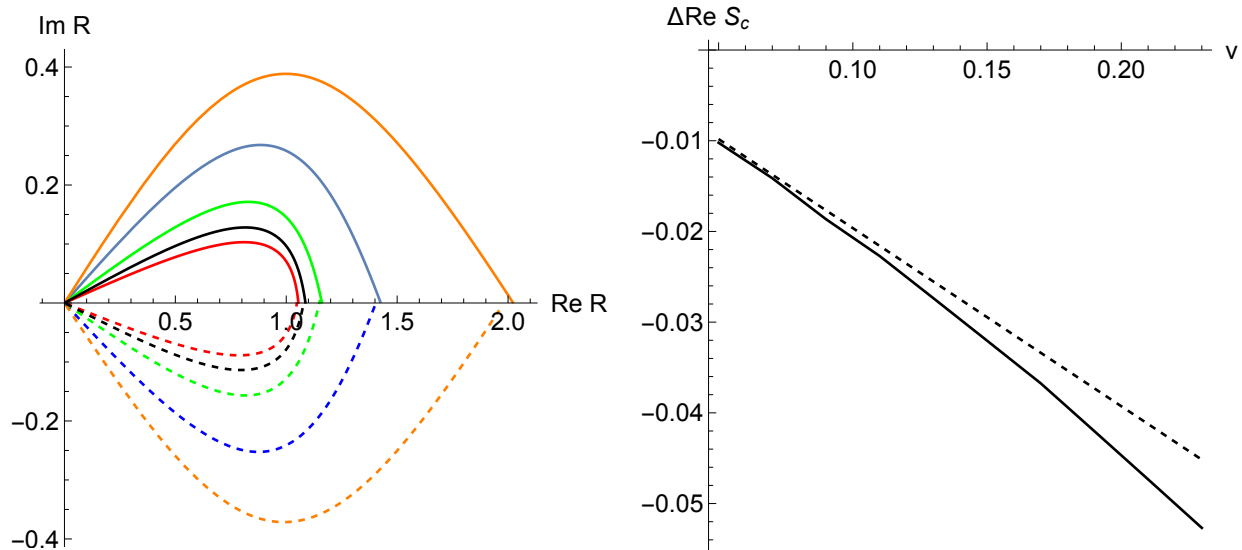


Figure 3: Left: Tunneling trajectories with $R_0 = 1$, $R_0 v_\sigma / \sigma = R_0 v_\epsilon / \epsilon = \frac{1}{20}$, and a range of γ between $-\pi/6$ and $-2\pi/3$. Right: the v -dependent correction to the real part of the on-shell action (solid) compared to the analytic result linearized in v (dashed, Eq. (38)), for $\gamma = -\pi/4$ and a range of v . (Here $\Delta \text{Re } S_c$ is normalized to $R_0^3 \sigma_0$ which controls the leading v -independent term in the on-shell action.)

In some cases, we can compute corrections to the tunneling exponent without knowledge of the full solution. Suppose that the parameters vary slowly enough that the linearizations (34) hold to a good approximation between $\tau = \tau_0$ and $\tau = 0$. The $\mathcal{O}(v_\epsilon, v_\sigma)$ corrections to the on-shell action are given by the $\mathcal{O}(v_\epsilon, v_\sigma)$ terms in the action evaluated on the $v_\epsilon = v_\sigma = 0$ solution, Eq. (13).³ We obtain:

$$\Delta \text{Re } S_c|_{\mathcal{O}(v)} = \frac{\pi}{4} \cot(\gamma) R_0^4 \left(v_\sigma - \frac{3}{4} R_0 v_\epsilon \right). \quad (37)$$

In Fig. 3 we compare the linear approximation to the full numerical result in some examples, finding agreement consistent with $\mathcal{O}(v^2)$ corrections.

As in the toy model studied in the previous section, we can map these solutions to wavepacket transition amplitudes as in (1). The solution begins at $R = 0$ at an initial $\tau = T_i$. The particle remains at rest at the origin until $\tau = \tau_0$, then moves to the nucleation point R_f at $T_f = 0$, where it possesses some final momentum p_f . The action is independent of T_i as long as $T_i < \tau_0$, and so we trivially continue the semiclassical amplitude e^{-S_c} back to real time, $T_i \rightarrow e^{-i\gamma} T_i$.

For fixed T_i , and assuming the barrier is growing monotonically sufficiently rapidly, the

³The reason is essentially the same as in the analysis of the toy model, Eq. (28). In the bulk time window the corrections to the solution itself only affect the action at $\mathcal{O}(v^2)$. The various boundary contributions either vanish because R vanishes at the initial time, or are purely imaginary because the final momentum for $v_{\epsilon, \sigma} = 0$ is real, cf. Eq. (15). Thus the entire $\mathcal{O}(v)$ correction to the real part of the action comes from the bulk $\mathcal{O}(v)$ term evaluated on the $v = 0$ solution (13).

largest tunneling amplitude corresponds to γ such that $\tau_0 = T_i$. For slow time dependence, this implies the relation $R_0 \csc \gamma \approx T_i$, and the correction to the tunneling exponent

$$\Delta \text{Re } S_c|_{\mathcal{O}(v), \text{max}} = -\frac{\pi}{4} \sqrt{T_i^2 - R_0^2 R_0^3} \left(v_\sigma - \frac{3}{4} R_0 v_\epsilon \right). \quad (38)$$

Again the correction (38) is easy to interpret. Part of the effect is translating the couplings σ_0 and ϵ_0 appearing in the leading time independent action, $\frac{\pi}{16} \sigma_0^4 / \epsilon_0^3$, back to the starting time T_i in the linearized approximation. This effect is dominant if $T_i \gg R_0$. The rest of the correction is the leading effect of time dependence while the particle is moving under the barrier. The former correction is captured by the replacements $\sigma_0 \rightarrow \sigma(t)$, $\epsilon_0 \rightarrow \epsilon(t)$, in the leading on-shell action at the linearized level. However, we see that this is an incomplete accounting of the $\mathcal{O}(v)$ terms, and corrections that arise from time dependence during the main part of barrier penetration are obtained in the more systematic analysis. The correction vanishes for the Euclidean case $T_i = R_0$ because the shift in the action is purely imaginary; this is a consequence of linearizing the time dependence, and nonzero corrections should be expected even in the Euclidean case if the time dependence is nonlinear.

More generally, the leading correction to the tunneling exponent should be obtained from the leading time-dependent perturbation to the time-independent action, integrated over the time-independent trajectories, and minimizing the real part over γ .

5 Coupling to gravity

In principle, the thin-wall bubble nucleation formalism used above may be extended to include gravitational effects. In static cases, like the thin-wall limit of (8), one can construct a suitable membrane effective action. We will discuss this case below and generalize slightly an effective action constructed by Visser [17]. The same action was used in [18] to compute decay rates in special cases using euclidean methods. In the presence of time-dependent driving fields, however, the construction of a complete membrane effective action is more cumbersome, and it is convenient to adopt some approximations. In one class of problems the gravitational field is the primary source of time dependence, and in favorable circumstances we can neglect the backreaction of the bubble on the gravitational field. In another class of problems the backreaction of the bubble on the field is accounted for, while the effects of time-dependent sources on the gravitational field can be neglected. We consider each case in turn.

As an example of the first type, suppose that we place the model (8) on a rigid FRW background, $ds^2 = -dt^2 + a(t)^2 dx_i^2$. Slow time dependence corresponds to tunneling processes that proceed quickly compared to the Hubble time a/\dot{a} . Suppose that we are interested in tunneling between times t_i and t_f , and we normalize the scale factor to 1 at t_f . Then we may set $a \approx 1 + H(t - t_f)$ where H is the Hubble parameter at t_f . To match to our framework in which tunneling ends at time zero, we shift the time coordinate, $t \rightarrow t + t_f$. Then

$$a = 1 + Ht \quad (39)$$

and the Klein-Gordon action expanded to $\mathcal{O}(H)$ is

$$S \approx \int d^4x [\mathcal{L}_{flat} + Ht(3\mathcal{L}_{flat} + (\partial_i\phi)^2)]. \quad (40)$$

The corresponding effective Lagrangian is

$$L = -(1 + 3Ht)\sigma R^2 \sqrt{1 - (\partial_t R)^2} + (1 + 3Ht)\epsilon R^3 + \frac{\sigma Ht R^2}{\sqrt{1 - (\partial_t R)^2}} \quad (41)$$

with σ and ϵ given by their flat-space values, $\sigma = 16\pi\sqrt{\lambda}a^3/3$ and $\epsilon = 4\pi\epsilon_0/3$. We see that in addition to time-dependent ϵ and σ , as in the model (31), there is also a new term.

The real part of the $\mathcal{O}(H)$ correction to the on-shell action, obtained from the $\mathcal{O}(H)$ term in Eq. (41), is found to vanish. In typical FRW spacetimes the acceleration is of order H^2 , so if there are $\mathcal{O}(H^2)$ corrections they must be found retaining both the acceleration and terms of order H^2 in the action and terms of order H in the solution. This problem can be studied numerically, but we will not pursue it further here.

Instead we consider another class of problems, where the gravitational field is static, but some gravitational backreaction from the bubble is incorporated. We start with the fully static problem. The Einstein-Hilbert action coupled to a brane is ⁴

$$S_{1,2}^{EHGH} = \frac{1}{16\pi G_N} \int_{\mathcal{M}_{1,2}} \sqrt{|g|} d^4x (\mathcal{R}_{1,2} - 2\Lambda_{1,2}) + \frac{1}{8\pi G_N} \int_{\mathcal{T}} \sqrt{|h|} d^3y K_{1,2} - \mu \int_{\mathcal{T}} \sqrt{|h|} d^3y, \quad (42)$$

where K is the trace of the extrinsic curvature tensor and \mathcal{T} denotes the brane worldvolume. The effective action for the location of the brane R is obtained by integrating out the bulk fields. We assume that the relevant true and false vacuum spacetimes are approximately de Sitter in the static slicing. The appropriate action is:

$$S_{\text{bubble}}^{\text{eff}} = \frac{4\pi}{8\pi G_N} \int d\lambda \left[2R\dot{R} \sinh^{-1} \left(\frac{\dot{R}}{\sigma_{dS_F} \sqrt{N^2 f_{dS_F}}} \right) - 2R\dot{R} \sinh^{-1} \left(\frac{\dot{R}}{\sigma_{dS_T} \sqrt{N^2 f_{dS_T}}} \right) + 2\sigma_{dS_T} R \sqrt{f_{dS_T} N^2 + \dot{R}^2} - 2\sigma_{dS_F} R \sqrt{f_{dS_F} N^2 + \dot{R}^2} - 8\pi G_N \mu N R^2 \right], \quad (43)$$

where $\dot{R} = \frac{dr}{d\lambda}$ and the subscripts T and F refer to the true and false vacua with $f_{dS_{T,F}} = 1 - R^2/L_{T,F}^2$. In general the value of each $\sigma_{dS_{T,F}}$ could be ± 1 . This action slightly generalizes that of Visser [17] (to which we refer for a more detailed derivation) by the inclusion of a metric degree of freedom on the brane, N which allows manifest reparametrization invariance.

⁴Other boundary terms besides \mathcal{T} will be neglected since they do not affect effective action.

Varying this degree of freedom, $\frac{\delta S_{bubble}}{\delta N} = 0$, we find ⁵

$$\sqrt{f_{dS_T} + N^{-2}\dot{R}^2} - \sqrt{f_{dS_F} + N^{-2}\dot{R}^2} - 4\pi\mu G_N R = 0. \quad (44)$$

The above equation is the only independent differential equation, since it turns out that the Euler-Lagrange equation obtained by varying r is simply the λ derivative of (44). Keeping the lapse in the action is important to obtain the first-order equation (44) from first principles. Having derived it as an Euler-Lagrange equation, we may now fix the gauge on the brane by setting $N = 1$, which identifies λ with the proper time s along worldlines of fixed angular coordinates on the brane. Then Eq. (44) matches the junction condition one would obtain by variation of the fields at \mathcal{T} in (42).

We now set $N = 1$ and continue $s \rightarrow e^{i\gamma'} s$. (We use γ' instead of γ because the proper time is not exactly the same as the coordinate time which was continued in earlier parts of this paper; we will derive the relationship below.) The energy is

$$E = e^{i\gamma'} \frac{\pi}{G_N} \left[R\sqrt{f_{dS_F} + e^{-2i\gamma'}\dot{R}^2} - R\sqrt{f_{dS_T} + e^{-2i\gamma'}\dot{R}^2} + 4\pi G_N \mu R^2 \right]. \quad (45)$$

Setting $N = 1$ and $s \rightarrow e^{i\gamma'} s$ into Eq. (44) we note that the energy vanishes on-shell, indicative of time reparametrization invariance. To find the classical solutions we first note that $R(s) = 0$ is a trivial solution with vanishing energy. To find the other solution branch we rearrange (44) into the form

$$e^{-2i\gamma'} \left(\frac{dR}{ds} \right)^2 + V(R) = 0, \quad (46)$$

where $V(R) = 1 - \alpha^2 R^2$, and $\alpha^2 = L_F^{-2} + \frac{(L_F^{-2} - L_T^{-2} - 16\pi^2 G_N^2 \mu^2)^2}{64\pi^2 G_N^2 \mu^2}$. The solution with vanishing energy at s_0 is

$$R(s) = \alpha^{-1} \cosh \left[\alpha e^{i\gamma'} (s - s_0) + i(\pi/2) \right]. \quad (47)$$

The initial proper time $s_0 = \frac{\pi}{2} \alpha^{-1} \csc(\gamma')$ is the largest negative time for which $\text{Im } R(0) = 0$. The final position at $s = 0$ is $R(0) = \alpha^{-1} \cosh((\pi/2) \cot \gamma')$ which falls within the classical allowed region $R > \alpha^{-1}$ for any γ' . Similar to the models of Sec. 3 the real time energy vanishes for the final position and momenta, and final states with different γ' are connected to each other at the classical level, by real time evolution. The on-shell action is given by the following integral $-i \int_{T_i}^{T_f} d\tau L_c = -i e^{i\gamma} \int_0^{R(0)} P(R) dR$, where $P(R)$ is the on-shell momenta

$$P(R) = \frac{1}{G_N} R \ln \left[\frac{\sqrt{1 - L_T^{-2} R^2}}{\sqrt{1 - L_F^{-2} R^2}} \left(\frac{\sqrt{\alpha^2 R^2 - 1} + R\sqrt{\alpha^2 - L_F^{-2}}}{\sqrt{\alpha^2 R^2 - 1} + R\sqrt{\alpha^2 - L_T^{-2}}} \right) \right]. \quad (48)$$

⁵We have chosen $\sigma_{dS_{T,F}} = +1$ which is the physically relevant case when $0 < R < L_F < L_T$, with same time orientation inside and outside the bubble, and for small enough positive μ . For an extensive analysis of different cases see [19] and references therein.

As one might expect the bubble action in Eq. (43) reduces to Eq. (7) with $p = 3$ to leading order in $R^2/G_N \rightarrow 0$ limit [18]. If we set $N = 1$ and expand (43) to leading order in G_N we find the following action

$$S_{\text{bubble}}^{\text{eff}} = \int ds \left(\frac{4}{3} \pi R^3 (\epsilon_F - \epsilon_T) \sqrt{1 + \dot{R}^2} - 4\pi\mu R^2 \right), \quad (49)$$

where $\Lambda_{T,F} = 3L_{T,F}^{-2} = 8\pi G_N \epsilon_{T,F}$ and \dot{R} means derivation with respect to proper time s . To match with (43) we also need to express the action in terms of the Lorentzian time t . To leading order in G_N the relation between s and t is usual time dilation relation $dt \approx ds \sqrt{1 + \left(\frac{dR}{ds}\right)^2}$. In terms of Lorentzian time t the Lagrangian of (49) is proportional to (43) with $p = 3$ and $R_0 = \frac{3\mu}{\epsilon_F - \epsilon_T} \approx \alpha^{-1}$.

Similarly we can recover the solution (13) from (47) in the $R^2/G_N \rightarrow 0$ limit. If we continue the time dilation relation we find

$$e^{i\gamma} d\tau \approx e^{i\gamma'} ds \sqrt{1 + e^{-2i\gamma'} \left(\frac{dR}{ds}\right)^2}. \quad (50)$$

If we now integrate the time dilation relation, use $\alpha^{-1} \approx R_0$ to leading order and the initial conditions s_0, τ_0 we find

$$e^{i\gamma} \tau - R_0 \cot \gamma = \alpha^{-1} \sinh \left(\alpha e^{i\gamma'} s - \frac{\pi}{2} \cot \gamma' \right). \quad (51)$$

Making use of (51) it is easy to check that the solution (47) reduces to (13). The relation between the coordinate time continuation parameter γ and the proper time parameter γ' can also be found, if we set $\tau = s = 0$ into (51). We find $\cot \gamma = \sinh \left(\frac{\pi}{2} \cot \gamma' \right)$, which together with (51) implies $R(0) = R_0 |\csc \gamma|$ as expected.

Now let us include some time dependence. A field theory model that can be mapped more or less straightforwardly to a time-dependent generalization of (43) is given by

$$V = \frac{1}{2} [\lambda_0 + (g/a)\chi] (\phi^2 - a^2)^2 - (\epsilon/2a)\phi + V_0 + V(\chi). \quad (52)$$

As in the nongravitational example, and for similar reasons, we consider the hierarchy $\lambda_0 a^4 \gg V_0 \gg (V(\chi), \epsilon) > 0$, so that the bubble profile is dominated by the ϕ^4 potential, and the state of the gravitational fields in the true and false vacua can be approximated by de Sitter space. We assume χ and ϕ are weakly coupled, which means both that g is small and that the metric in the bubble background does not substantially alter the background solution for χ , which is consistent with the small ϵ approximation.

The relevant rolling solution for χ at $\mathcal{O}(g^0)$ is homogeneous in the flat slicing of dS. The static slicing is more convenient for the present problem, so χ is a function of the form $\chi(t + L \log \sqrt{1 - r^2/L^2})$, with $L^2 \approx 3M_p^2/V_0$ and r and t the static radial and time coordinates, respectively.

This model is obviously not the most general case, since the background spacetimes are approximated as time-independent and the underlying field theory model is certainly fine-tuned. Its main virtue is that the effective action is almost entirely recycled from the time-independent case. In the thin-wall limit the bubble dynamics of the model (52) maps to a membrane effective action of the form (43) with $\mu \rightarrow \mu(t_{dS_F}, R)$. The spacetime dependence of the tension appears at $\mathcal{O}(g)$ and is inherited from the background solution for χ in static coordinates.

If we set lapse variation of (43) to zero with μ time dependent, rearrange and apply a λ derivative on both sides we find

$$\frac{d}{d\lambda} \left[\frac{R}{\left(\frac{\partial q}{\partial N}\right)} \left(2\sqrt{f_{dS_T} + N^{-2}\dot{R}^2} - 2\sqrt{f_{dS_F} + N^{-2}\dot{R}^2} - \tilde{\mu}R \right) \right] = -NR^2 \frac{\partial \tilde{\mu}}{\partial t_{dS_F}}, \quad (53)$$

where we defined $q := \sqrt{f_{dS_F}^{-1}N^2 + f_{dS_F}^{-2}\dot{R}^2}$ and $\tilde{\mu} := 8\pi G_N \mu$. Eq. (44) is a first order equation analogous to a conservation of energy law. Eq. (53) is a second order equation describing the non-conservation of energy by the varying μ .

From this point one may proceed to rotate the time contour and seek suitable tunneling solutions connecting the vacuum to nucleated bubble states. Similarly to the nongravitational cases, at leading order (in the derivative of μ with respect to the flat time slicing) corrections to the tunneling probability may be found from the unperturbed solutions (47) and extremization over γ .

6 An instanton in a Kaluza-Klein cosmology

We conclude with an example where an exact solution of the field equations in a time-dependent background may be obtained. The setting is purely gravitational and describes tunneling in a certain Kaluza-Klein cosmology. We begin with the metric

$$ds^2 = -dy^2 + y^2 d\phi^2 + dt^2 + dx^2 + x^2 d\psi^2, \quad (54)$$

with timelike coordinate y and non-standard Kaluza-Klein identification

$$(t, \phi) \sim \left(t + 2\pi n \frac{\mu}{\sqrt{\mu - a^2}}, \phi - 2\pi n \frac{a}{\sqrt{\mu - a^2}} \right) \quad (55)$$

and $0 \leq a^2 \leq \mu$. For nonzero a the KK circle is twisted with spatial Milne-type coordinate ϕ . Indeed, the metric (54) can be extended in a similar way to the Milne extension to Minkowski. First we define

$$\tilde{\phi} = \phi + (a/\mu)t. \quad (56)$$

At fixed $\tilde{\phi}$ the periodicity is simply $t \sim t + 2\pi n \frac{\mu}{\sqrt{\mu-a^2}}$. We then transform $y^2 = z^2 - w^2$, $\tanh \tilde{\phi} = z/w$ to obtain

$$ds^2 = -dz^2 + \left(1 + \frac{a^2}{\mu^2}(z^2 - w^2)\right) dt^2 + \frac{2a}{\mu} dt(wdz - zdw) + dw^2 + dx^2 + x^2 d\psi^2. \quad (57)$$

This will play the role of our vacuum spacetime. Locally, it is just flat space, but globally there is a KK circle with interesting properties. For $a = 0$, (57) is ordinary KK spacetime which can decay by nucleating a bubble of nothing [20]. The instanton is the Euclidean continuation of 5D Schwarzschild-Tangherlini. For nonzero a , the vacuum spacetime is more exotic: it is cylindrically symmetric, time dependent, and exhibits a Killing horizon for ∂_t at $w^2 = w_s^2 \equiv z^2 + \mu^2/a^2$, beyond which the KK circles are closed timelike curves (CTCs). The presences of CTCs is certainly an upsetting feature, and we will assume that (57) is only valid out to some cutoff \bar{w}^2 , with

$$\bar{w}^2 < w_s^2, \quad (58)$$

beyond which the spacetime is “completed” in a more physical way. (This is clearly a strong assumption. We will see at least a physical argument below that for $a^2 \ll \mu$ there is a parametric separation between the spacetime region supporting bubble nucleation and the region exhibiting CTCs, lending some support to the idea that the regions can be studied independently.) The most interesting feature is that for $w^2 < w_s^2$ the proper circumference of the KK circle is time (z) dependent, shrinking to a minimum size $2\pi \sqrt{\frac{\mu^2 - a^2 w^2}{\mu - a^2}}$ at $z = 0$. Then an explicit instanton solution describing the decay of this approximate spacetime may be obtained by analytic continuation of a Myers-Perry black hole [21].⁶

The 5D Myers-Perry solution with one nonzero angular momentum parameter is given in Boyer-Lindquist-type coordinates by the Lorentzian metric

$$ds^2 = -dt^2 + \sin^2 \theta (r^2 + a^2) d\phi^2 + \frac{\mu}{\rho^2} (dt + a \sin^2 \theta d\phi)^2 + \frac{\rho^2}{r^2 + a^2 - \mu} dr^2 + \rho^2 d\theta^2 + r^2 \cos^2 \theta d\psi^2, \quad (59)$$

where $\rho^2 = r^2 + a^2 \cos^2 \theta$, $a^2 < \mu$, and the horizon is at $r_H = \sqrt{\mu - a^2}$. Let us review the limiting behaviors. Asymptotically, the metric takes the form

$$ds^2 = -dt^2 + dr^2 + r^2 (d\theta^2 + \sin^2 \theta d\phi^2 + \cos^2 \theta d\psi^2). \quad (60)$$

The angular part describes an S^3 in “Hopf” coordinates. ϕ, ψ range from 0 to 2π and θ ranges from 0 to $\pi/2$. Next we inspect the near-horizon limit, following the notation of [22]. Define the Killing vector $\ell = \partial_t - (a/\mu)\partial_\phi$. Then the horizon is a fixed surface of ℓ , $\ell^2|_{r_H} = 0$. Introducing the coordinate $\tilde{\phi} = \phi + (a/\mu)t$ as above, which is constant on the orbits of ℓ , the

⁶Ref. [22] also studied continuations of Myers-Perry solutions. We will differ in the choice of continuation, and therefore also in the interpretation.

near-horizon metric at fixed $\theta, \tilde{\phi}, \psi$ takes the form

$$ds^2 = 2(\mu - a^2 \sin^2 \theta) \left(-\frac{r_H}{\mu^2} (r - r_H) dt^2 + \frac{1}{4r_H} \frac{dr^2}{r - r_H} \right), \quad (61)$$

and in terms of a proper radial coordinate v it is proportional to

$$ds^2 = dv^2 - v^2 \left(\frac{\mu - a^2}{\mu^2} \right) dt^2. \quad (62)$$

Now we perform the analytic continuation

$$t \rightarrow it, \quad \phi \rightarrow i\phi, \quad \theta \rightarrow i\theta. \quad (63)$$

Under this map θ and ϕ become noncompact, and θ becomes timelike. The continued metric is

$$ds^2 = \frac{r^2 + a^2 \cosh^2 \theta}{r^2 + a^2 - \mu} dr^2 + dt^2 - \frac{\mu}{r^2 + a^2 \cosh^2 \theta} (dt - a \sinh^2 \theta d\phi)^2 + r^2 \left(- \left[1 + \frac{a^2 \cosh^2 \theta}{r^2} \right] d\theta^2 + \sinh^2 \theta \left[1 + \frac{a^2}{r^2} \right] d\phi^2 + \cosh^2 \theta d\psi^2 \right). \quad (64)$$

Asymptotically in r it behaves as

$$ds^2 = dr^2 + dt^2 + r^2 (-d\theta^2 + \sinh^2 \theta d\phi^2 + \cosh^2 \theta d\psi^2). \quad (65)$$

Transforming $\tanh^2 \theta = (z^2 - w^2)/x^2$, $r^2 = x^2 - z^2 + w^2$, $\tanh \tilde{\phi} = z/w$, we recover the vacuum metric (57). The periodicities also match, as can be seen from the continuation of the near-horizon metric (62). Absence of a conical singularity at $r = r_H$ implies the periodicity $t \sim t + 2\pi \frac{\mu}{\sqrt{\mu - a^2}}$ at fixed $\tilde{\phi}$. Then in terms of the original coordinates we recover precisely the periodicity (55). We also conclude that the radial coordinate is bounded, $r \geq r_H$, capping off smoothly at $r = r_H$.

Thus the spacetime (64) describes something bubble-like embedded in the cosmology (57). The induced metric on the bubble wall worldvolume $r \rightarrow r_H$ is

$$ds^2 = -(\mu + a^2 \sinh^2 \theta) d\theta^2 + (\mu - a^2) \cosh^2 \theta d\psi^2 + \frac{\mu^2 \sinh^2 \theta}{\mu + a^2 \sinh^2 \theta} d\tilde{\phi}^2 \quad (66)$$

which is somewhat opaque. On the wall we make the coordinate transformation

$$\begin{aligned} \sinh \tau &= \sinh \theta \cosh \tilde{\phi} \\ \cosh \tau \cos \chi &= \sinh \theta \sinh \tilde{\phi}. \end{aligned} \quad (67)$$

τ is a timelike coordinate on the wall, and the induced metric at fixed τ becomes, to $\mathcal{O}(a^2)$,

$$ds^2 = \cosh^2 \tau \left[\left(\mu + \frac{a^2}{4} ((\cos 2\chi - 1) \cosh 2\tau - (3 \cos 2\chi + 1)) \right) d\chi^2 + (\mu - a^2) \sin^2(\chi) d\psi^2 \right]. \quad (68)$$

At $\tau = 0$ it has the form of the induced metric on a prolate spheroid embedded in \mathbb{R}^3 , in spherical coordinates with polar angle χ and azimuthal angle ψ , and ratio of semi-axis lengths $c/b = 1/\sqrt{1 - a^2/\mu}$. It expands exponentially and deforms as time evolves.

To summarize, after the continuation (63), the 5D black hole becomes a Lorentzian geometry corresponding to an expanding bubble, embedded in a KK space with nonstandard identification of the KK circle. It is therefore a candidate decay product for the classical solution (57). More precisely, since we assume the solution (57) is only valid for $w^2 < \bar{w}^2 \ll (\mu/a)^2$, we have a candidate decay product so long as the bubble fits, $r_H^2 \ll \bar{w}^2$. For small a the cutoff must fall between $\mu \ll \bar{w}^2 < (\mu/a)^2$.

Is there a saddle point of the gravitational action with action S , such that the leading order decay amplitude is $e^{-Re(S)}$?

Because the black hole is stationary instead of static, there is no real Euclidean section that can be obtained by analytic continuation of the coordinates alone. We may obtain a suitable candidate from (59) by making the $\tilde{\phi} = \phi + (a/\mu)t$ substitution and continuing only $t \rightarrow it$. The result is a “quasi-Euclidean” metric with a bubble wall at $r = r_H$ and the Euclidean vacuum, Eq. (57) with $z \rightarrow -iz$, at large radius $\sqrt{x^2 + w^2}$. The induced metric on the $z = 0$ nucleation hypersurface agrees between the quasi-Euclidean instanton and the Lorentzian nucleated bubble 64.

The action of the quasi-Euclidean solution is

$$S = \frac{\pi^2 \mu^2}{G_5 \sqrt{\mu - a^2}}. \quad (69)$$

It recovers the action of Witten’s bubble in the limit $a \rightarrow 0$ and diverges in the extremal limit $a \rightarrow \sqrt{\mu}$, where the KK circle size diverges.

The quasi-Euclidean solution describes the amplitude to evolve from a state with no bubble at some early time z_i to a state with a bubble at some late time z_f . The action controls the amplitude for the bubble to nucleate, and the analytic continuation describes the subsequent bubble evolution. Since the background is time dependent there is no time translation symmetry and the instanton computes a probability rather than a rate. Note that the transition occurs when the KK circle is smallest near the origin of the spatial coordinates. This corresponds to the smallest potential barrier.

We conclude this section with a few comments.

- The bubble of nothing example studied in this section is similar to previous examples we have seen, in that it involves a saddle point off in the complexified phase space. Quasi-euclidean metrics based on the continuation of Kerr-like solutions are known to

play a variety of useful other roles [23, 24].

- In a few other ways, the present example is different. First, the presence of a time reversal symmetry means there is a time when the quasi-Euclidean solution returns to the real axis with zero momentum. (Indeed, in the notation of previous sections we have only considered the Euclidean continuation $\gamma = -\pi/2$.) Also, we have only found an explicit solution when the initial time is early, so that the KK circle is shrinking, and the final time is late, when it is expanding again. In previous examples we were able to find families of instantons for more general initial and final times. Finally, the bubble is neither thin wall nor spherically symmetric. In all other cases, the background was rotationally invariant and the bubble was thin-wall and spherical by assumption.
- At first sight, a more natural starting point would be the background (54) with standard periodicity $\phi \sim \phi + 2\pi$. However, this spacetime is singular at $y = 0$, where the circle shrinks to zero size. The instanton in this case is also singular and has zero action – there is no barrier to tunneling at this moment. The purpose of the twisted periodicity is to regulate the circle so that it is never smaller than $\mu/\sqrt{\mu - a^2}$ at the origin.

7 Discussion

We have surveyed the effects of slow explicit time dependence on barrier penetration and bubble nucleation in some simple models. The problem is interesting not because the effects are typically dramatic, but because the usual semiclassical techniques require some development in order to calculate the effects. It appears to be useful generalize the Wick rotation to other contours in the complex time plane, which provides semiclassical access to different tunneling times during a fixed time window. “Nucleation,” in the sense of the bubble in the final state, need not occur at rest, and semiclassical trajectories with nonzero final momentum can be interpreted as providing a saddle point solution for a path integral with wavepacket initial and final states, with the real and imaginary parts of the final momentum mapping to phases and gradients of the wavepacket.

Reduction to effective quantum mechanical models simplified the problem enormously, essentially from a nonlinear PDE back to a nonlinear ODE, as one has in the fully field-theoretic treatment of $O(4)$ -symmetric problems. It is unclear if there is a practical generalization of our methods to full field theories, although in some favorable cases exact solutions can be guessed.

We conclude with a few directions for future work. First, our analysis was entirely at the leading semiclassical order. The fluctuation determinant has interesting technical features, requiring the solution of flow equations to identify suitable middle-dimensional integration cycles [25].

Second, in the effective model of membrane nucleation coupled to gravity, the construction of the effective action itself is somewhat nontrivial, and we only illustrated the construction in some relatively simple classes of models. Further analysis and generalization could be of interest for cosmological applications.

Finally, our study of exact solutions was limited to a single example. Some continuations of other black hole and black ring solutions in higher dimensions presumably describe bubble of nothing decays in more exotic Kaluza-Klein cosmologies, and it would be interesting to catalog them.

Acknowledgements

We thank Szilard Farkas, Adam Nahum, LianTao Wang, and Yikun Wang for useful discussions. This work was supported in part by the U.S. Department of Energy, Office of Science, Office of High Energy Physics under award number DE-SC0015655.

References

- [1] S. Coleman, “Fate of the false vacuum: Semiclassical theory,” *Phys. Rev. D* **15** (May, 1977) 2929–2936. <https://link.aps.org/doi/10.1103/PhysRevD.15.2929>.
- [2] C. G. Callan, Jr. and S. R. Coleman, “The Fate of the False Vacuum. 2. First Quantum Corrections,” *Phys. Rev. D* **16** (1977) 1762–1768.
- [3] S. R. Coleman and F. De Luccia, “Gravitational Effects on and of Vacuum Decay,” *Phys. Rev. D* **21** (1980) 3305.
- [4] A. Andreassen, D. Farhi, W. Frost, and M. D. Schwartz, “Precision decay rate calculations in quantum field theory,” *Phys. Rev. D* **95** (Apr, 2017) 085011. <https://link.aps.org/doi/10.1103/PhysRevD.95.085011>.
- [5] J. R. Espinosa, “A Fresh Look at the Calculation of Tunneling Actions,” *JCAP* **07** (2018) 036, [arXiv:1805.03680](https://arxiv.org/abs/1805.03680) [[hep-th](#)].
- [6] J. Braden, M. C. Johnson, H. V. Peiris, A. Pontzen, and S. Weinfurtner, “New Semiclassical Picture of Vacuum Decay,” *Phys. Rev. Lett.* **123** no. 3, (2019) 031601, [arXiv:1806.06069](https://arxiv.org/abs/1806.06069) [[hep-th](#)]. [Erratum: *Phys.Rev.Lett.* 129, 059901 (2022)].
- [7] V. Guada and M. Nemevšek, “Exact one-loop false vacuum decay rate,” *Phys. Rev. D* **102** (2020) 125017, [arXiv:2009.01535](https://arxiv.org/abs/2009.01535) [[hep-th](#)].
- [8] W.-Y. Ai and M. Drewes, “Schwinger effect and false vacuum decay as quantum-mechanical tunneling of a relativistic particle,” *Phys. Rev. D* **102** no. 7, (2020) 076015, [arXiv:2005.14163](https://arxiv.org/abs/2005.14163) [[hep-th](#)].
- [9] G. Lagnese, F. M. Surace, M. Kormos, and P. Calabrese, “False vacuum decay in quantum spin chains,” *Phys. Rev. B* **104** no. 20, (2021) L201106, [arXiv:2107.10176](https://arxiv.org/abs/2107.10176) [[cond-mat.stat-mech](#)].

- [10] T. Hayashi, K. Kamada, N. Oshita, and J. Yokoyama, “Vacuum decay in the Lorentzian path integral,” *JCAP* **05** no. 05, (2022) 041, [arXiv:2112.09284 \[hep-th\]](#).
- [11] H. Matsui, “Lorentzian path integral for quantum tunneling and WKB approximation for wave-function,” *Eur. Phys. J. C* **82** no. 5, (2022) 426, [arXiv:2102.09767 \[gr-qc\]](#).
- [12] D. Croon, E. Hall, and H. Murayama, “Non-perturbative methods for false vacuum decay,” [arXiv:2104.10687 \[hep-th\]](#).
- [13] A. Ivanov, A. Ivanov, M. Matteini, M. Matteini, M. Nemevšek, M. Nemevšek, L. Ubaldi, and L. Ubaldi, “Analytic thin wall false vacuum decay rate,” *JHEP* **03** (2022) 209, [arXiv:2202.04498 \[hep-th\]](#). [Erratum: JHEP 07, 085 (2022), Erratum: JHEP 11, 157 (2022)].
- [14] S. P. de Alwis, “Revisiting Vacuum decay in Field Theory,” [arXiv:2305.11786 \[hep-th\]](#).
- [15] J. Schiff, Y. Goldfarb, and D. J. Tannor, “Path-integral derivations of complex trajectory methods,” *Phys. Rev. A* **83** (Jan, 2011) 012104. <https://link.aps.org/doi/10.1103/PhysRevA.83.012104>.
- [16] A. Cherman and M. Unsal, “Real-Time Feynman Path Integral Realization of Instantons,” [arXiv:1408.0012 \[hep-th\]](#).
- [17] M. Visser, “Quantum wormholes,” *Phys. Rev. D* **43** (1991) 402–409.
- [18] S. Ansoldi, A. Aurilla, R. Balbinot, and E. Spallucci, “Effective dynamics of self-gravitating extended objects,” *Physics Essays* **9** no. 4, (Jan., 1996) 556–562, [arXiv:gr-qc/9707001 \[gr-qc\]](#).
- [19] S. V. Chernov and V. I. Dokuchaev, “Vacuum shell in the Schwarzschild-de Sitter world,” *Class. Quant. Grav.* **25** (2008) 015004, [arXiv:0709.0616 \[gr-qc\]](#).
- [20] E. Witten, “Instability of the Kaluza-Klein Vacuum,” *Nucl. Phys. B* **195** (1982) 481–492.
- [21] R. C. Myers and M. J. Perry, “Black Holes in Higher Dimensional Space-Times,” *Annals Phys.* **172** (1986) 304.
- [22] F. Dowker, J. P. Gauntlett, G. W. Gibbons, and G. T. Horowitz, “The Decay of magnetic fields in Kaluza-Klein theory,” *Phys. Rev. D* **52** (1995) 6929–6940, [arXiv:hep-th/9507143](#).
- [23] R. Monteiro, M. J. Perry, and J. E. Santos, “Thermodynamic instability of rotating black holes,” *Phys. Rev. D* **80** (2009) 024041, [arXiv:0903.3256 \[gr-qc\]](#).
- [24] E. Witten, “A Note On Complex Spacetime Metrics,” [arXiv:2111.06514 \[hep-th\]](#).
- [25] E. Witten, “A New Look At The Path Integral Of Quantum Mechanics,” [arXiv:1009.6032 \[hep-th\]](#).